

# Trends in the global tropopause thickness revealed by radiosondes

Sha Feng,<sup>1,2</sup> Yunfei Fu,<sup>1</sup> and Qingnong Xiao<sup>3</sup>

Received 7 August 2012; revised 11 September 2012; accepted 18 September 2012; published 20 October 2012.

[1] The first global trends in the thickness of the tropopause layer (TL) are analyzed based on radiosonde data in the Integrated Global Radiosonde Archive (IGRA) for the period of 1965–2004. It reveals that TL has been thickening for the entire globe with positive trends of  $0.16 \pm 0.12$  km/decade during this period. Statistically significant thickening is observed in the tropics, North Hemisphere (NH) extratropics, and NH poles. Accompanied by overall cooling of  $-0.58 \pm 0.40$  K/decade in TL's top, remarkable rising trends of  $0.35 \pm 0.29$  km/decade are observed in the corresponding height. However, the anti-correlation of the trends in the tropopause temperature and the corresponding height is not observed in its lower boundary, namely the first lapse rate tropopause (LRT), for all the latitude bands as suggested by the previous studies. The results imply that the temperature of the TL is primarily couple with the height of its upper boundary as the thickness of the TL is more correlated with the temperature of the lower stratosphere than with the temperature of the upper troposphere. Long-term changes in TL may in turn carry more information how tropopause change in response to climate change than in the sharp “tropopause surface” only. **Citation:** Feng, S., Y. Fu, and Q. Xiao (2012), Trends in the global tropopause thickness revealed by radiosondes, *Geophys. Res. Lett.*, 39, L20706, doi:10.1029/2012GL053460.

## 1. Introduction

[2] Over the past decades, it has become clear that tropopause is an atmosphere layer, rather than a sharp surface, that is between troposphere and stratosphere and has properties of both the troposphere and the stratosphere. Owing to its extreme sensitivity to climate variability and climate change, tropopause itself has attracted much research interest [Fueglistaler et al., 2009; Gettelman et al., 2007, 2011; Hoinka, 1998; Santer et al., 2003; Zängl and Hoinka, 2001]. The growing evidence from a variety of data sources has suggested that the height of the tropopause has increased in the last decades [Santer et al., 2003; Sausen and Santer, 2003; Seidel and Randel, 2006], which is closely associated with tropospheric warming and stratospheric cooling [Añel et al., 2006; Santer et al., 2004]. Santer et al. [2003]

revealed that global tropopause pressure decreased by 2.16 hPa/decade in the NCEP reanalysis for 1979–2000 and by 1.13 hPa/decade in the ECWMF reanalysis for 1979–1993. Using radiosonde data for the period of 1980–2004, Seidel and Randel [2006] also indicated upward tropopause height trends of  $64 \pm 21$  m/decade with a corresponding tropopause pressure trend of  $-1.7 \pm 0.6$  hPa/decade. However, the trends they concluded were only on the basis of a sharp “tropopause surface” derived from the first lapse rate tropopause (LRT) [WMO, 1957]. To date, no study has reported the trends in the entire tropopause layer (TL), i.e. its thickness and upper and lower boundaries.

[3] Using the WMO criterion, temperature profiles often exhibit multiple surfaces to fit the criterion, which has been described as “multiple tropopause (MT) events” [Añel et al., 2007, 2008; Randel et al., 2007; Schmidt et al., 2006]. Considering the first and last LRT as the bottom and top of TL, Schmidt et al. [2006] estimated the geographical and temporal distribution of the thickness of TL for the entire globe using GPS observation, and found consistent conclusions with Pan et al. [2004], who examined the extratropical tropopause from the perspective of chemical composition. This definition is applied in this study for climatological statistics of TL. We attempt to estimate seasonal variation and long-term linear trends in the thickness and the vertical boundaries of global TL using radiosonde observations in the Integrated Global Radiosonde Archive (IGRA). The IGRA data offer substantially higher vertical resolution than reanalyses plus much longer records than GPS radio occultations, thus allowing a more accurate identification of the tropopause and possible multiple tropopause levels from a climatic perspective.

[4] Section 2 outlines the radiosonde data used and discusses the tropopause definition. Section 3 describes the latitudinal structure, seasonal variation, and long-term trends of the TL. Section 4 provides discussions and concluding remarks.

## 2. Data and Methods

[5] The IGRA, consisting of over 1,500 globally distributed radiosonde stations, is the most comprehensive and the largest radiosonde dataset. It combines radiosonde and pilot balloon observations, and quality control algorithms have been applied to remove gross errors [Añel et al., 2007; Durre et al., 2006, 2008]. Given that many of the records are short or incomplete, our analyses relied on the meteorological sounding profiles of a subset of 187 stations (hereafter S187) reported in the IGRA from 1965 to 2004, of which the spatial homogeneity and temporal coverage were extensively discussed and analyzed by the previous studies [Añel et al., 2007, 2008; Antuña et al., 2006; Wallis, 1998]. Furthermore, we only considered the soundings reaching 70 hPa to

<sup>1</sup>Laboratory of Satellite Remote Sensing and Climate Environment, School of Earth and Space Sciences, University of Science and Technology of China, Anhui, China.

<sup>2</sup>College of Marine Science, University of South Florida, St. Petersburg, Florida, USA.

<sup>3</sup>Center for Severe Weather Research, Boulder, Colorado, USA.

Corresponding author: Y. Fu, Laboratory of Satellite Remote Sensing and Climate Environment, School of Earth and Space Sciences, University of Science and Technology of China, Hefei, Anhui 230026, China. (fyf@ustc.edu.cn)

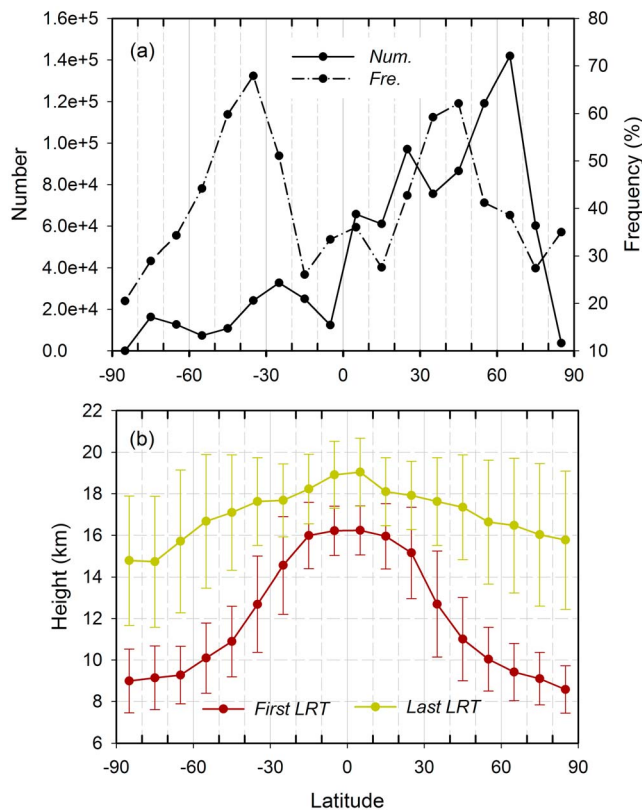


**Figure 1.** Latitudinal distribution of (a) number of soundings (solid line) and frequency of MT events (dashed line) and (b) average height of the bottom (red: first LRT) and top (yellow: last LRT) of TL. Error bars indicate  $\pm 1$  standard deviation about the tropopause height.

assure that all of them have the same opportunity to detect MT events.

[6] We applied the WMO criterion to all available soundings of S187, using the tropopause detection algorithm that was proposed by Reichler *et al.* [2003]. In the WMO criterion [WMO, 1957], “The first tropopause is defined as the lowest level at which the lapse rate  $\Gamma = -\partial_z T$  (where  $T$  is temperature) decreases to  $2^\circ\text{C}/\text{km}$  or less, provided also the averaged lapse rate between this level and all higher levels within 2 km does not exceed  $2^\circ\text{C}/\text{km}$ . If above the first tropopause the average lapse rate between any level and all higher levels within 1 km exceeds  $3^\circ\text{C}/\text{km}$ , then a second tropopause is defined by the same criterion as above. This tropopause may be either within or above the 1 km layer.” Here our main interest is in the climatological feature of the thickness of TL, which is determined by  $\Delta(LRT_{\text{last}} - LRT_{\text{first}})$ , on the global scale [Schmidt *et al.*, 2006]. To avoid unreal tropopause detections, the LRT above 40 hPa or below 500 hPa was removed. All tropopause heights stated in this study refer to the geopotential heights.

[7] The seasonal variation of TL parameters was computed by averaging all available soundings for each calendar month. Trend calculations were on the basis of monthly anomalies that were estimated by subtracting the annual cycle from each individual monthly mean. For the determination of trend uncertainties, the confidence interval of 95% was calculated using a  $t$  test. If both the lower and upper

limits of the interval for the trends are with the same sign, the trend is statistically significant.

### 3. Results

#### 3.1. Latitudinal Structure of TL

[8] For the complete period from 1965 to 2004, a total number of 862,965 soundings were available for S187, of which 42.46% occurred MT events. Figure 1a presents the number of soundings and frequency of MT per  $10^\circ$  in latitude. Clearly, the Northern Hemisphere (NH) extratropics is the best sampled region where a large number of stations perform four soundings per day instead of two [Añel *et al.*, 2007]. The frequency of MT shows a nearly symmetric behavior between the Northern and Southern Hemispheres (SH) with local maxima in the vicinity of the subtropical jet stream regions ( $30^\circ$ – $50^\circ$ ), which has been demonstrated well by previous studies [Añel *et al.*, 2008; Pan *et al.*, 2004; Randel *et al.*, 2007; Schmidt *et al.*, 2006; Seidel and Randel, 2006].

[9] For comparison with the previous studies, the climatological statistics of TL’s bottom, namely first LRT, was based on all available soundings in this study. As expected, either the top or the bottom of TL is higher over the equatorial region and descends poleward (Figure 1b). The height of TL’s bottom decreases from 16.2 km near the equator ( $10^\circ\text{S}$ – $10^\circ\text{N}$ ) to  $\sim 8.5$  km over the polar regions. The strong gradient in the height of TL’s bottom occurs between  $20^\circ$  and  $50^\circ$  on both hemispheres. The TL’s top shows the similar latitudinal variation as the bottom but with the smaller range from 15 km over equator to 19 km over poles. As a consequence, the climatological thickness of TL becomes thicker from 2.6 km to  $\sim 7$  km with latitude increment. Figure 1b also presents the standard deviations of the vertical boundary height of TL, which are smallest between  $20^\circ\text{S}$  and  $20^\circ\text{N}$ . The maximum standard deviations of the TL’s bottom ( $\sim 2$  km) occur between  $20^\circ$  and  $50^\circ$  on both hemispheres for the shift of subtropical jet streams [Añel *et al.*, 2008; Bischoff *et al.*, 2007; Feng *et al.*, 2011; Randel *et al.*, 2007; Schmidt *et al.*, 2005, 2006]. The reason for the large standard deviation of TL’s top height need to be further examined, and we do not further discuss it in this study.

[10] In terms of the latitudinal feature of TL, five latitude bands were determined to the tropics ( $20^\circ\text{S}$ – $20^\circ\text{N}$ ), SH extratropics ( $20^\circ\text{S}$ – $50^\circ\text{S}$ ), NH extratropics ( $20^\circ\text{N}$ – $50^\circ\text{N}$ ), SH poles ( $50^\circ\text{S}$ – $90^\circ\text{S}$ ), and NH poles ( $50^\circ\text{N}$ – $90^\circ\text{N}$ ) for further discussion. In the following sections, we will focus on the climatological statistics of TL for each latitude bands. We also compared the results with those from  $30^\circ$ -latitude bands as each region, which showed the same overall patterns as obtained in this study. Besides, an excellent agreement was exhibited in the well-sampled regions, i.e. the tropics and NH extratropics.

#### 3.2. Seasonal Variation

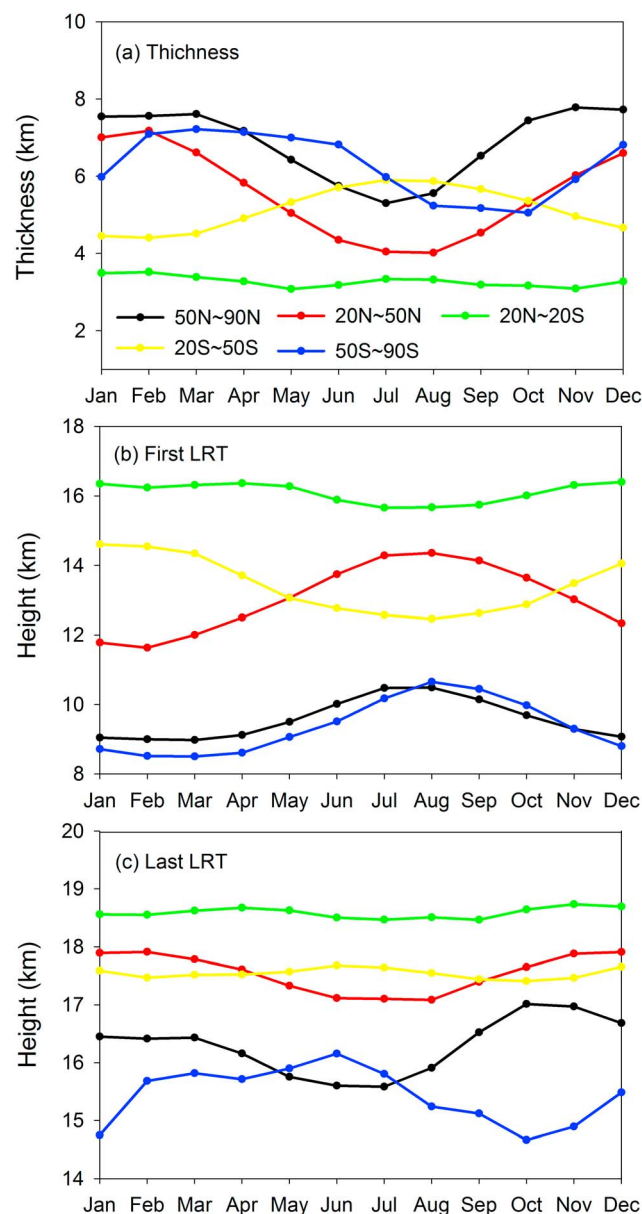
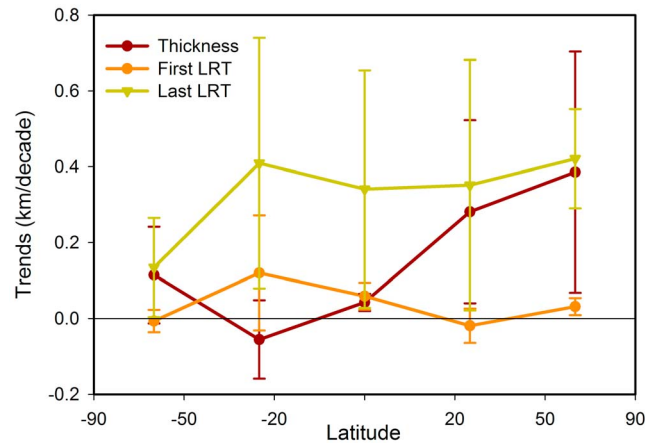
[11] Table 1 summarizes the seasonal frequency of MT occurring in each latitude band. All the regions have near or more than one third of MT occurrence except both poles in the respective summer. With the intensified subtropical jet stream in the respective winter, MT occurrence reaches maxima with the frequency of over 60% for extratropics of both hemispheres, as already pointed out in Section 3.1.

**Table 1.** Seasonal Frequency of MT Events With Respect to Soundings in Each Latitude Band<sup>a</sup>

	50°N–90°N	20°N–50°N	20°N–20°S	20°S–50°S	50°S–90°S
DJF	46.58	66.79	29.56	49.51	19.79
MAM	35.55	60.55	29.76	55.31	33.75
JJA	26.99	40.09	33.77	65.71	46.59
SON	42.40	49.18	30.49	62.53	31.32

<sup>a</sup>DJF represents December–January–February; MAM represents March–April–May; JJA represents June–July–August; SON represents September–October–November.

[12] Averaging time series from the stations in each latitude band to reduce the noises and increase the statistical significance, the monthly mean of the thickness and the height of vertical boundaries of TL are analyzed for the five latitude bands. The thickness of TL shows strong seasonal

**Figure 2.** Monthly mean of (a) the thickness and the height of the (b) bottom and (c) top of TL.**Figure 3.** Trends in zonal-mean thickness (brown) and the height of the top (yellow: last LRT) and bottom (orange: first LRT) of TL. Error bars indicate the 95% confidence interval for the trend estimates.

variation in the extratropics and the poles but not in the tropics (Figure 2a) due to smooth seasonal variation of both top and bottom of the TL (Figures 2b and 2c). For the specific latitude band, NH extratropics exhibit the strongest seasonal variation of TL thickness ranging from  $\sim 4$  km in JJA to  $\sim 7$  km in DJF, while SH extratropics present the opposite variation from  $\sim 4.5$  km in JJA to  $\sim 6$  km DJF. The climatological thickness of TL for the extratropics ranges from 4.9 km to 6.3 km corresponding to 105–144 hPa in pressure, which is consistent well with the typical values of 105–175 hPa achieved by *Añel et al.* [2008]. NH poles have the thickest ( $\sim 7.7$  km) TL in DJF and the thinnest ( $\sim 5.5$  km) in JJA, while SH poles have a phase lag of seasonal variation of TL thickness with the NH one. Attributing to the similar seasonal variation of the bottom height of TL in SH poles, it turns to be thinnest ( $\sim 5$  km) in SON and thickest ( $\sim 7.2$  km) in MAM. The phenomenon that seasonal variation of the thickness of the TL for SH poles is in phase of the one for NH poles may arise from the data quality and homogeneity issues, because we have only 14 stations providing time series that contribute to the climatological mean for SH poles where the results could be interpreted inaccurately because of the lack of stations.

### 3.3. Trends in TL

[13] Figure 3 shows the linear trends in TL during 1965–2004, and Figure 4 shows the monthly anomalies of the temperature and height of the TL's vertical boundaries. Basically, the height of TL's lower boundary (first LRT) has smaller trend confidence intervals for all latitude bands, which was determined by all available soundings in each latitude band, whereas the thickness and the upper boundary of TL were only determined when the MT event appears.

[14] Figure 3 presents a significant increase in the height of TL's top for all latitude bands ranging from 0.13 to 0.42 km/decade, yielding a net rise of  $0.35 \pm 0.29$  km/decade over 40 years, that were accompanied by overall significant cooling of  $-0.58 \pm 0.40$  K/decade in the corresponding temperatures (Figure 4b).

[15] However, the positive trends in the height of the bottom of TL are observed only over SH extratropics,

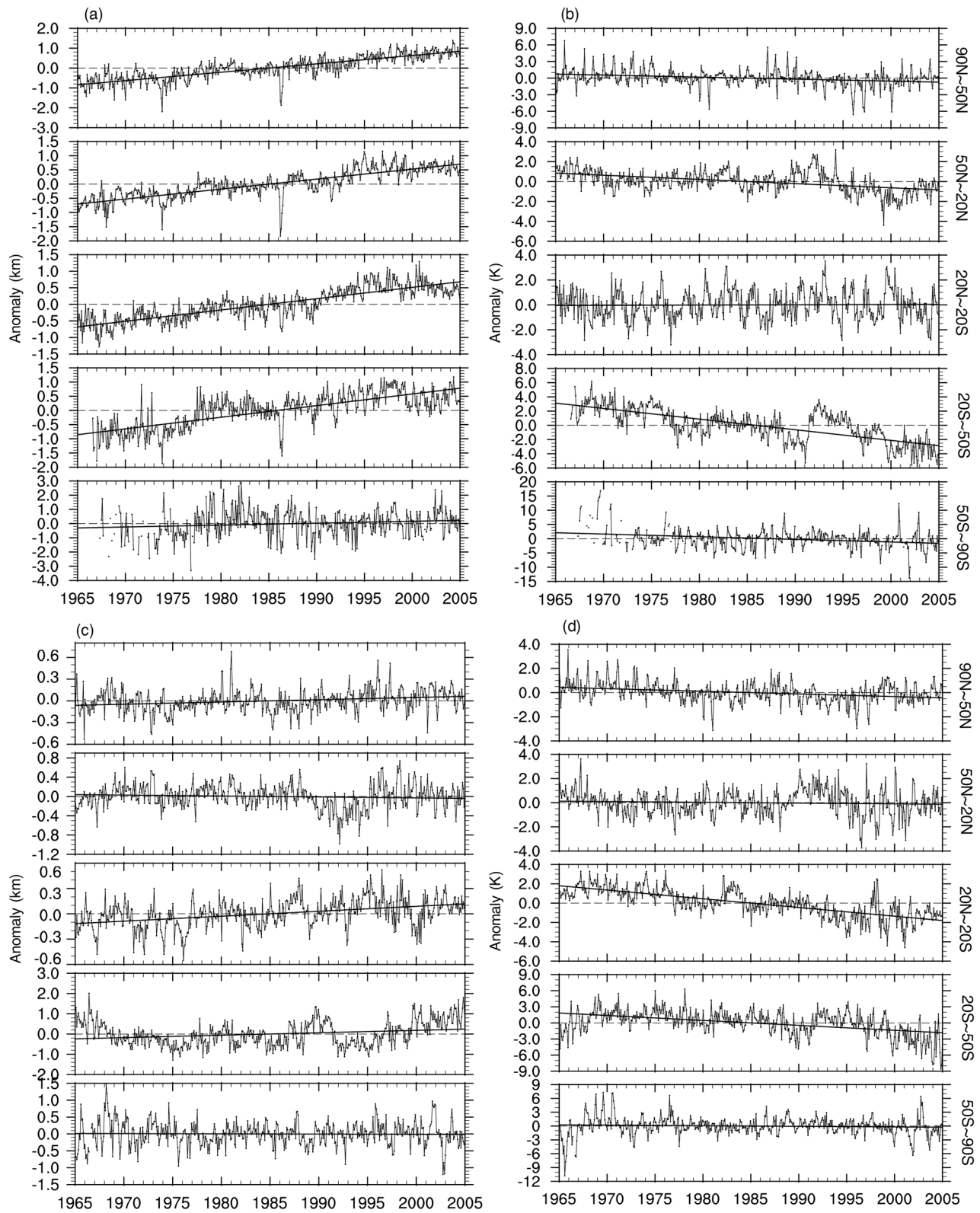


**Figure 4.** Monthly anomalies of temperature (Figures 4b and 4d) and height (Figures 4a and 4c) of the (a and b) top and (c and d) bottom of TL for the five latitude bands during 1965–2004. Thick solid lines are fitted linear trends with a least-square procedure.

tropics, and NH poles but not over SH poles and NH extratropics where the negative trends are against the results of *Seidel and Randel* [2006]. *Seidel and Randel* [2006] indicated positive trends in the first LRT for all zones during 1980 to 2004. The large negative anomalies of the first LRT height for NH extratropics during 1987 to 1995 (Figure 4c) may account for an increase height if only taking into account the period of 1980–2004 for the trend calculation. For supporting our assumption, we derived the trends in the first LRT height from the available soundings for the period of 1980 to 2004. The net global rise of  $0.09 \pm 0.07$  km/decade has a good agreement with *Seidel and Randel* [2006]. In addition, we also calculated the global trends ( $-1.03$  hPa/decade) for the first LRT in pressure, which shows an excellent agreement with previous studies [*Santer et al.*, 2003; *Seidel and Randel*, 2006]. However, the significant anti-correlation between the tropopause temperature and the corresponding height pointed out by the previous studies [*Añel et al.*, 2006; *Santer et al.*, 2004; *Seidel and Randel*, 2006] were not observed in all regions for the bottom of TL but only in NH poles and tropics.

[16] For the entire TL, Figure 3 shows significant thickening in NH and tropics, with the positive trends of  $0.39 \pm 0.31$  km/decade for NH poles,  $0.28 \pm 0.24$  km/decade for NH extratropics, and  $0.04 \pm 0.02$  km/decade for tropics, slight but not statistically significant thickening over SH poles ( $0.12 \pm 0.12$  km/decade), and slight but not statistically significant thinning over SH extratropics ( $-0.06 \pm 0.10$  km/decade). Overall, the increases in the height of both top and bottom of TL for SH extratropics, tropics, and NH poles infer a rise of the entire TL over these regions.

#### 4. Discussion and Conclusions

[17] The first global trends in the thickness of the TL were presented by analyzing sounding reports of S187 in the IGRA from 1965 to 2004 in this study. The analysis also includes the latitudinal distribution, seasonal variation, and long-term linear trend of TL thickness and its vertical boundaries.

[18] A total number of 862,965 soundings were available for this period, of which 42.46% occur MT events using the WMO criterion. With the intensified subtropical jet stream in winter, the extratropics on both hemispheres have the most frequent occurrence of MT events with the frequency over 60%. *Schmidt et al.* [2006] found that GPS data exhibit about twice MT occurrence and the TL thickness by reanalysis data in the subtropical jet stream regions. Apparently, higher-resolution radiosondes are supposed to be much better for resolving the climatological features near the tropopause [*Davis and Emanuel*, 1991; *Randel et al.*, 2007].

[19] Considering the first and the last LRT as the lower (bottom) and upper (top) boundaries of TL, the TL becomes thinnest near the equator and thickest over the polar regions. Its thickness shows strong seasonal variation in the extratropics and poles but not in the tropics. NH extratropics has minimum thickness of  $\sim 4$  km in JJA and maximum value of  $\sim 7$  km in DJF. On the other hand, the TL over NH poles and SH extratropics is the thickest in the respective winter but the thinnest in the respective summer as well. The one for SH poles shows in phase with its NH counterpart.

[20] A net thickening of  $0.16 \pm 0.12$  km/decade for the global TL was obtained due to the positive trends in the thickness of the TL almost for all the latitude bands. The statistically significant thickening is observed in the TL over NH extratropics, NH poles, and the tropics with linear trends of  $0.28 \pm 0.24$  km/decade,  $0.39 \pm 0.31$  km/decade, and  $0.04 \pm 0.02$  km/decade, respectively. The positive trends in the TL's thickness may associated with the significant positive trends in the frequency of double tropopause events in radiosonde data, which proved an increase of upper tropospheric and lower stratospheric wave baroclinicity [*Castanheira et al.*, 2009].

[21] Accompanied by overall cooling of  $-0.58 \pm 0.40$  K/decade, the top of TL shows overall remarkable rising trends of  $0.35 \pm 0.29$  km/decade for the studied period. The significantly positive trends were presented in the bottom of TL for the tropics, NH poles, and SH extratropics, inferring a rise of the entire TL over these regions. However, the anti-correlation of the trends in the tropopause temperature and the corresponding height that was suggested by previous studies were not consistently exhibited in the bottom of TL but only in its top as the thickness of the TL is more correlated with the temperature of the lower stratosphere than with the temperature of the upper troposphere, implying long-term change in TL may carry more information how tropopause change in response to climate change than only in “tropopause surface” that is defined by the first LRT.

[22] **Acknowledgments.** We would like to thank National Oceanic and Atmospheric Administration (NOAA) for supplying Integrated Global Radiosonde Archive (IGRA) data set and Juan A. Añel and Torsten Schmidt for their helpful comments and suggestions. We thank three anonymous reviewers whose comments led us to improve the original manuscript. This work is funded by National Basic Research Program of China (973 program, grant 2010CB428601), the Knowledge Innovation Program of the Chinese Academy of Sciences (grant KZCX2-YW-Q11-04) and NSFC (40730950, 41075041).

[23] The Editor thanks two anonymous reviewers for assistance evaluating this manuscript.

#### References

- Añel, J. A., L. Gimeno, L. de la Torre, and R. Nieto (2006), Changes in tropopause height for the Eurasian region determined from CARDS radiosonde data, *Naturwissenschaften*, 93(12), 603–609, doi:10.1007/s00114-006-0147-5.
- Añel, J. A., J. C. Antuña, L. de la Torre, R. Nieto, and L. Gimeno (2007), Global statistics of multiple tropopauses from the IGRA database, *Geophys. Res. Lett.*, 34, L06709, doi:10.1029/2006GL029224.
- Añel, J. A., J. C. Antuña, L. de la Torre, J. M. Castanheira, and L. Gimeno (2008), Climatological features of global multiple tropopause events, *J. Geophys. Res.*, 113, D00B08, doi:10.1029/2007JD009697.
- Antuña, J. C., J. A. Añel, and L. Gimeno (2006), Impact of missing sounding reports on mandatory levels and tropopause statistics: a case study, *Ann. Geophys.*, 24(10), 2445–2449, doi:10.5194/angeo-24-2445-2006.
- Bischoff, S. A., P. O. Canziani, and A. E. Yuchechen (2007), The tropopause at southern extratropical latitudes: Argentine operational rawinsonde climatology, *Int. J. Climatol.*, 27(2), 189–209, doi:10.1002/joc.1385.
- Castanheira, J. M., J. A. Añel, C. A. F. Marques, J. C. Antuña, M. L. R. Liberato, L. de la Torre, and L. Gimeno (2009), Increase of upper troposphere/lower stratosphere wave baroclinicity during the second half of the 20th century, *Atmos. Chem. Phys.*, 9(23), 9143–9153, doi:10.5194/acp-9-9143-2009.
- Davis, C. A., and K. A. Emanuel (1991), Potential vorticity diagnostics of cyclogenesis, *Mon. Weather Rev.*, 119(8), 1929–1953, doi:10.1175/1520-0493(1991)119<1929:PVD0C>2.0.CO;2.
- Durre, I., R. S. Vose, and D. B. Wuertz (2006), Overview of the integrated global radiosonde archive, *J. Clim.*, 19(1), 53–68, doi:10.1175/JCLI3594.1.
- Durre, I., R. S. Vose, and D. B. Wuertz (2008), Robust automated quality assurance of radiosonde temperatures, *J. Appl. Meteorol. Climatol.*, 47(8), 2081–2095, doi:10.1175/2008JAMC1809.1.



- Feng, S., Y. Fu, and Q. Xiao (2011), Is the tropopause higher over the Tibetan Plateau? Observational evidence from Constellation Observing System for Meteorology, Ionosphere, and Climate (COSMIC) data, *J. Geophys. Res.*, **116**, D21121, doi:10.1029/2011JD016140.
- Fueglistaler, S., A. E. Dessler, T. J. Dunkerton, I. Folkins, Q. Fu, and P. W. Mote (2009), Tropical tropopause layer, *Rev. Geophys.*, **47**, RG1004, doi:10.1029/2008RG000267.
- Gettelman, A., M. A. Geller, and P. H. Haynes (2007), A SPARC tropopause initiative, *SPARC Newsl.*, **29**, 14–20.
- Gettelman, A., P. Hoor, L. L. Pan, W. J. Randel, M. I. Hegglin, and T. Birner (2011), The extratropical upper troposphere and lower stratosphere, *Rev. Geophys.*, **49**, RG3003, doi:10.1029/2011RG000355.
- Hoinka, K. P. (1998), Statistics of the global tropopause pressure, *Mon. Weather Rev.*, **126**(12), 3303–3325, doi:10.1175/1520-0493(1998)126<3303:SOTGTP>2.0.CO;2.
- Pan, L. L., W. J. Randel, B. L. Gary, M. J. Mahoney, and E. J. Hints (2004), Definitions and sharpness of the extratropical tropopause: A trace gas perspective, *J. Geophys. Res.*, **109**, D23103, doi:10.1029/2004JD004982.
- Randel, W. J., D. J. Seidel, and L. L. Pan (2007), Observational characteristics of double tropopauses, *J. Geophys. Res.*, **112**, D07309, doi:10.1029/2006JD007904.
- Reichler, T., M. Dameris, and R. Sausen (2003), Determining the tropopause height from gridded data, *Geophys. Res. Lett.*, **30**(20), 2042, doi:10.1029/2003GL018240.
- Santer, B. D., et al. (2003), Behavior of tropopause height and atmospheric temperature in models, reanalyses, and observations: Decadal changes, *J. Geophys. Res.*, **108**(D1), 4002, doi:10.1029/2002JD002258.
- Santer, B. D., et al. (2004), Identification of anthropogenic climate change using a second-generation reanalysis, *J. Geophys. Res.*, **109**, D21104, doi:10.1029/2004JD005075.
- Sausen, R., and D. Santer (2003), Use of changes in tropopause height to detect influences on climate, *Meteorol. Z.*, **12**(3), 131–136, doi:10.1127/0941-2948/2003/0012-0131.
- Schmidt, T., S. Heise, J. Wickert, G. Beyerle, and C. Reigber (2005), GPS radio occultation with CHAMP and SAC-C: Global monitoring of thermal tropopause parameters, *Atmos. Chem. Phys.*, **5**(6), 1473–1488, doi:10.5194/acp-5-1473-2005.
- Schmidt, T., G. Beyerle, S. Heise, J. Wickert, and M. Rothacher (2006), A climatology of multiple tropopauses derived from GPS radio occultations with CHAMP and SAC-C, *Geophys. Res. Lett.*, **33**, L04808, doi:10.1029/2005GL024600.
- Seidel, D. J., and W. J. Randel (2006), Variability and trends in the global tropopause estimated from radiosonde data, *J. Geophys. Res.*, **111**, D21101, doi:10.1029/2006JD007363.
- Wallis, T. W. R. (1998), A subset of core stations from the Comprehensive Aerological Reference Dataset (CARDS), *J. Clim.*, **11**(2), 272–282, doi:10.1175/1520-0442(1998)011<0272:ASOCSE>2.0.CO;2.
- WMO (1957), Meteorology: A three-dimensional science: Second session of the Commission for Aerology, *WMO Bull.*, **4**, 134–138.
- Zängl, G., and K. P. Hoinka (2001), The tropopause in the polar regions, *J. Clim.*, **14**(14), 3117–3139, doi:10.1175/1520-0442(2001)014<3117:TTITPR>2.0.CO;2.